

OPTIMIZATION INVESTIGATION ON THE GEOMETRICAL PARAMETERS OF A SCRUBBER USING GENETIC ALGORITHM

Jiarui Wang^{1&}, Simin Wang^{1&*}, Chen Song¹, and Zaoxiao Zhang^{1*}

¹ School of Chemical Engineering and Technology, Xi'an Jiaotong University, Xi'an 710049, China

[&] These authors contributed to the work equally and should be regarded as co-first authors

* Corresponding Author: smwang@xjtu.edu.cn, zhangzx@mail.xjtu.edu.cn

ABSTRACT

The wet scrubber can be used for reducing particles and recover waste heat from flue gas, but its particle removal performance is relatively poor. To improve its performance, an effective algorithm combining genetic aggregation response surface method with multi-objective genetic algorithm was adopted to study the effects of geometrical parameters. Based on particle scavenging model, a gas-liquid-solid three phase numerical method was adopted to simulate the process of wet scrubbing. The particle removal efficiency, heat transfer efficiency and pressure drop were considered as objective functions. After response surface analysis, the local sensitivity and a set of Pareto-optimal points were obtained. The results show that the response surface results have a good agreement with simulation data and the particle removal efficiency and temperature drop of optimized structure can be increased by 4.66% and 17.42%, respectively, which provides guidelines for engineering applications.

Keywords: gas-liquid-solid multiphase flow; scrubber; numerical simulation; optimization

NONMENCLATURE

Abbreviations

MOGA Multi-Objective Genetic Algorithm

Symbols

C_c the Cunningham slip correction factor
 C_d the drag coefficient
 d diameter, μ m
 D the scrubber diameter, m
 D_{diff} the diffusion coefficient of particle
 E the collection efficiency

E_i	the impact energy of droplets
k	turbulence pulsation kinetic-energy, $m^2 \cdot s^{-2}$
k_B	the Boltzmann constant, $J \cdot K^{-1}$
K_R	interception parameter
P	pressure, Pa
Pe	Peclet number
Re	Reynolds number
Stk	Stokes number
T	temperature, K
u_i	velocity in x, y, z direction, $m \cdot s^{-1}$
v	velocity magnitude, $m \cdot s^{-1}$
ϵ	Turbulent pulsating kinetic energy dissipation rate, $kg \cdot m^{-1} \cdot s^{-1}$
μ	dynamic viscosity, Pa·s
η	the particle removal efficiency
θ	the spray angle, °
ρ	fluid density, $kg \cdot m^{-3}$
σ	surface tension, $N \cdot m^{-1}$

Subscript

g, d, p gas, droplets, particles

1. INTRODUCTION

Wet scrubbing method can remove particles from gas, meanwhile, a scrubber can also be used as a direct contact heat exchanger to recover waste heat. Therefore, there may be a synergistic effect between pollutant control and waste heat recovery which are both hot issues in the chemical industry. This paper mainly focuses on this synergistic effect, especially on fine particle reduction.

A lot of studies on the performance of the wet scrubber have been conducted. For the particles with the aerodynamic diameters larger than $50\mu m$, the removal efficiency could reach almost 100% in a wet scrubber [1].

While the particle removal efficiencies were 28.7% for PM1 and of 39.6% for PM2.5 in a 1000-MW power plant [2]. But most of them are concentrated on the effects of operating parameters. Mohan et al carried out the experiment on the performance of a spray tower for removal of fine particulate matter under different operating conditions and develop a correlation to quantify the performance of the tower [3]. Wu et al investigated the effects of dust particle diameters, inlet concentrations of dust particles, and the flow rates of gas and liquid of a spray scrubber on particle removal efficiency using the experimental and modelling approaches [4]. Pan et al conducted experiments to study the relationship between entrainment of slurry droplets and emitted fine particles and the effects of operating parameters on droplet and fine particle emissions [5]. To enhance the performance of spray scrubbers, Lotfi et al. used woodchips as a packing material in a lab scale wet scrubber and studied the effects of oil/gas ratio, oil temperature and woodchips size on the tar model compounds removal from producer gas [6]. Jafari et al developed an open scrubbing tower through optimization of the parameters including nozzle type, number of stages of spray nozzle, operating pressure and inlet NH₃ concentration [7]. Chen et al. investigated the types of scrubbing tower, i.e. open scrubbing tower, scrubbing tower with porous tray and scrubbing tower with a flow pattern control device on a pilot-scale experimental setup [8]. Comparing to that of open scrubbing tower, the removal efficiency was improved by 13% for the scrubbing tower with a flow pattern control device.

The particle removal performance of wet scrubber depends on the capture capacity of droplets, which is mainly governed by the inertial collision, interception and diffusion mechanisms. Cheng et al. also estimated collection efficiency of a spray scrubber by a correlation. And they made assumptions such as a constant flue gas velocity and impaction efficiency of a single droplet with particles, a single scrubbing liquid droplet size, no wall-film and ignoring the effects of turbulence to simply the calculation [9]. But these assumptions can adversely affect the accuracy of predictions. Mohebbi et al. established a two-dimensional mathematical model to predict the particle removal efficiency in an orifice scrubber using inertial collision theory [10]. The effect of operating parameters such as gas velocity, liquid to gas flow rate ratio and particle diameter were obtained. Majid et al. also simulated the characteristic of multiphase flow in a venturi scrubber based on inertial

collision theory. Throat gas velocity, gas volume fraction, droplet size and removal efficiency were investigated [11]. Lim et al. explored the effects of several parameters on overall collection efficiency numerically based on impaction, interception and diffusion mechanisms in a reverse jet scrubber, such as liquid droplet diameter, relative velocity of liquid droplet and gas stream, packing density, and particle diameter, and so on [12].

The present study aimed to optimize a laboratory scale spray scrubber using response surface analysis and Multi-Objective Genetic Algorithm (MOGA). Numerical simulation for a laboratory scale spray scrubber was conducted in this work using the Euler approach to predict the gas flow and particle concentration, the Lagrange approach for droplets movement and the user defined function codes to simulate the droplet-particle interactions. The particle removal efficiency was validated by comparison with published data.

2. GEOMETRIC STRUCTURE AND MATHEMATICAL METHOD

2.1 Geometric model and boundary condition

The schematic diagram of a typical spray scrubber is shown in Fig. 1. The temperature of air and droplet at inlets are 300.15K and 293.15K, respectively. The relative humidity of air at inlet is 78%. The spray flux of water and air velocity are 2kg/s, 0.5m/s, respectively. And the diameters of initial droplet and particle are 0.4mm, 10μm, respectively. These operating conditions are obtained through optimization calculation. As shown in Fig. 1, three geometrical parameters are investigated, such as the height of the sprayer (h), the diameter of scrubber (D) and the cone angle (θ).

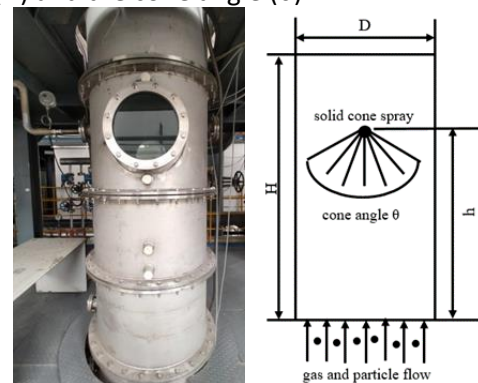


Fig.1 The schematic diagram of a typical open scrubbing tower

The finite volume method was adopted to resolve the conservation equations. The Green-Gauss Node-Based method was applied to calculate the gradients. The quick scheme was used to discretize the momentum

equation, energy equation and turbulence equations. The movement equations for droplets were calculated by the Runge-Kutta method.

2.2 liquid droplets movement and evaporation

The motions of liquid droplets are simulated in the Lagrange approach. As it is impossible to compute the trajectory of every individual particle, the parcels are used in the numerical simulation. Each parcel represents a number of liquid droplets with equal locations, velocity, diameter and temperature. The equations to calculate the movement of the droplets can be written as:

$$\frac{d\vec{v}_d}{dt} = \frac{(\rho_d - \rho_g)\vec{g}}{\rho_d} + \frac{\vec{v}_g - \vec{v}_d}{\tau_r} \quad (1)$$

$$\tau_r = \frac{\rho_d d_d^2}{18\mu_g C_d Re} \quad (2)$$

where C_d is the droplet drag coefficient.

$$C_d = C_{d,sphere} (1 + 2.632y) \quad (3)$$

$$C_{d,sphere} = \begin{cases} 0.424 & Re > 1000 \\ \frac{24}{Re} (1 + \frac{1}{6} Re^{2/3}) & Re < 1000 \end{cases} \quad (4)$$

$$\frac{d^2 y}{dt^2} = \frac{C_F}{C_b} \frac{\rho_g}{\rho_d} \frac{v_{rel}^2}{r^2} - \frac{C_k \sigma}{\rho_d r^3} y - \frac{C_l \mu_d}{\rho_d r^2} \frac{dy}{dt} \quad (5)$$

Where C_F, C_b, C_k, C_l are 1/3, 1/2, 8, 5, respectively.

In this work, the rate of vaporization can be assumed to be governed by gradient diffusion:

$$\Delta m_d = N_i A_d M \Delta t \quad (6)$$

$$N_i = k_c (C_{i,s} - C_{i,\infty}) \quad (7)$$

where N_i is the molar flux of vapor, k_c is the mass transfer coefficient, $C_{i,s}$ is the vapor concentration at the droplet surface, $C_{i,\infty}$ is the vapor concentration in the bulk gas.

The mass transfer coefficient k_c is calculated from the Sherwood number correlation:

$$Sh_{AB} = \frac{k_c d_d}{D_{i,m}} = 2.0 + 0.6 Re^{1/2} Sc^{1/3} \quad (8)$$

The droplet temperature is updated as:

$$m_d c_p \frac{dT_d}{dt} = h A_d (T_\infty - T_d) - \frac{dm_d}{dt} L \quad (9)$$

where h is the convective heat transfer coefficient, L is the latent heat.

The convective heat transfer coefficient h is calculated with a modified Nu number as follows:

$$Nu = \frac{h d_d}{k} = 2.0 + 0.6 Re^{1/2} Pr^{1/3} \quad (10)$$

where k is the thermal conductivity of the continuous phase, Pr is the Prandtl number of the continuous phase.

2.3 Particle scavenging model

Collection efficiency E is the ability of a droplet to collide with the dust particles and scavenge particles within the droplet volume. The mechanisms of particle scavenging mainly involve impaction, interception, diffusion. The particle collection efficiency by a single droplet due to impaction can be calculated by the following equation:

$$E_I = \left(\frac{Stk}{Stk + 1} \right)^r \quad (11)$$

$$Stk = \frac{v_{rel} d_p^2 \rho_p}{18 \mu_g d_d} \quad (12)$$

$$r = 0.759 Stk^{-0.245} \quad (13)$$

The collection efficiency of interception is defined as (Hao et al. 1989) :

$$E_R = (1 + K_R)^2 - \frac{3}{2} (1 + K_R) + \frac{1}{2(1 + K_R)} \quad (14)$$

where K_R is the dimensionless parameter describing the interception effect, $K_R = \frac{d_p}{d_d}$.

The diffusive collection efficiency is given by (Hao et al. 1989) :

$$E_D = 8/Pe + 2.23 Re_d^{1/8} Pe^{-5/8} \quad (15)$$

where Pe is the Peclet number defined as:

$$Pe = \frac{d_d v_{rel}}{D_{diff}} \quad (16)$$

where D_{diff} the diffusion coefficient of particle is defined as:

$$D_{diff} = \frac{k_B T C_c}{3\pi\mu d_p} \quad (17)$$

Thus, the overall collection efficiency can be written as (Davenport et al. 1978) :

$$E = 1 - (1 - E_I)(1 - E_R)(1 - E_D) \quad (18)$$

2.4 Model validation

In order to validate the accuracy of numerical model and solution method, a numerical model was set up according to Tomb's experiment device and simulation results were compared with the experimental data from Tomb (Tomb et al. 1972). As shown in Figs.2, the results illustrate that the particle removal efficiency obtained from numerical simulation are in good agreement with the experimental results. Hence, it can be concluded that the numerical method is reliable. The differences may be

caused by simplification of physical model and boundary conditions in simulation, and unavoidable measurement error in experiment.

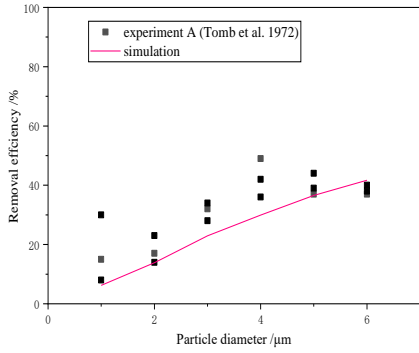


Fig.2 Comparison of the particle removal efficiency between numerical results and experimental data

2.5 Optimization method

In this paper, three geometrical parameters were set as input parameters and particle removal efficiency, pressure drop and temperature drop were set as output parameters. A set of design points was generated by the central composite design which was characterized by its high efficiency and good predictability. Then the Genetic Aggregation response surface was applied in order to investigate the relationship of the input parameters and output parameters. The Genetic Aggregation response surface automates the process of selecting, configuring, and generating the type of response surface best suited to each output parameter. According to above description, the ranges of input parameters of this study are shown in table 1 and the objective functions are as follows:

$$\text{Maximum: } \eta = \frac{C_{p,inlet} - C_{p,outlet}}{C_{p,inlet}} \quad (19)$$

$$\text{Maximum: } \Delta T = T_{inlet} - T_{outlet} \quad (20)$$

$$\text{Minimum: } \Delta P = P_{inlet} - P_{outlet} \quad (21)$$

where η is the overall particle removal efficiency, C is the particle concentration, ΔP is the pressure drop.

Table 1 The range of input parameters

Input parameters	Value range
Height of sprayer h	1-3m
Diameter of scrubber D	0.5-2m
Cone angle θ	60-160°

3. RESULTS AND DISCUSSION

3.1 Goodness of fit

The goodness of fit for output parameters can be displayed in Fig.3. The coefficient of determination R^2 is an important criterion to evaluate the accuracy of

response surface model, which can be mathematically represented as:

$$R^2 = 1 - \frac{\sum_{i=1}^n (y_i - \hat{y}_i)^2}{\sum_{i=1}^n (y_i - \bar{y})^2} \quad (22)$$

Where y_i is the value of output variables at the i -th design point, \bar{y} is the arithmetic mean of the values of y_i , and \hat{y}_i is the value of response surface at the i -th design point.

The values of R^2 for η , ΔP and ΔT are 97.62%, 99.57% and 99.25%, respectively. The best value of the coefficient of determination R^2 is 100%. Hence, the response surface model can be accurately obtained by design points. The results show that the values predicted from response agree well with the values calculated at design points.

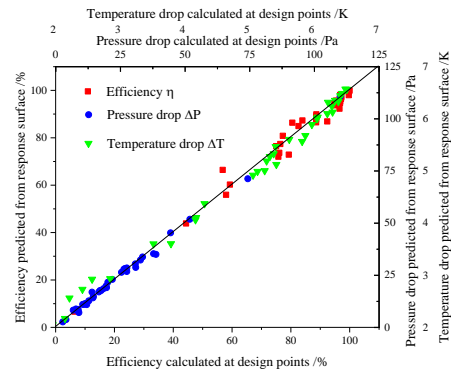


Fig.3 The goodness of fit for output parameters

3.2 Effects of the sprayer height

The effects of the sprayer height on particle removal efficiency, pressure drop, temperature drop are shown in Fig.4. When the height increases from 1 m to 3 m, the particle removal efficiency increases by 3.31%, the pressure drop increases by 56.21% and the temperature drop increases by 62.47% where the diameter of scrubber, spray angle are 1m, 100°, respectively. When the height reaches 2.5m, the particle removal efficiency and temperature drop almost stabilizes, but the pressure drop still increases rapidly. For one thing the resident time of particles increases with the increase of the height of sprayer. For another thing the relative velocity between particle and droplets decrease as droplets drop down which makes the collection efficiency of droplets smaller. And the phenomenon of gas flow deflection gets serious with the increase of the height of sprayer which causes particles escape.

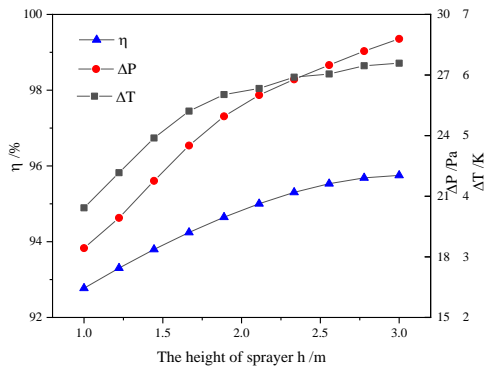


Fig.4 Effects of the sprayer height on output parameters

3.3 Effects of the scrubber diameter

The effects of scrubber diameter are shown in Fig.5 where the sprayer height and spray angle are 2m, 100°, respectively. When the scrubber diameter varies from 0.5 to 3.0m, the particle removal efficiency decreases by 42.5%, the pressure drop decreases by 89.78% and the temperature drop decreases by 72.32%, respectively. This reveals that the scrubber diameter has a greater influence than the sprayer height. Larger scrubber diameter means smaller droplet velocity near walls and the collection efficiency of these droplets and air flow resistance near walls reduces quickly.

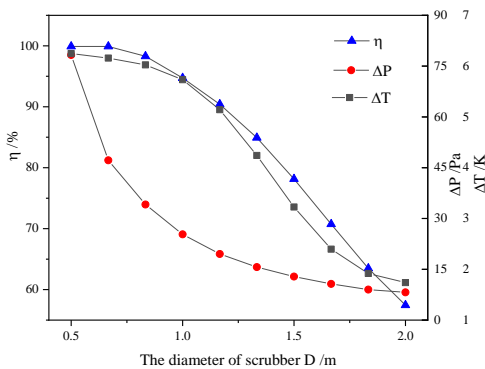


Fig.5 Effects of the scrubber diameter on output parameters

With the increase of scrubber diameter, the air flow rate increases and air trends to flow through the areas near walls. Thus, this part of fluid could not contact with droplets adequately and the temperature drop decreases drastically.

3.4 Effects of the spray angle

The effects of scrubber diameter are shown in Fig.6 where the sprayer height and spray angle are 2m, 100°, respectively. When the scrubber diameter varies from 0.5 to 3.0m, the particle removal efficiency decreases by 42.5%, the pressure drop decreases by 89.78% and the temperature drop decreases by 72.32%, respectively.

This reveals that the scrubber diameter has a greater influence than the sprayer height. Larger scrubber diameter means smaller droplet velocity near walls and the collection efficiency of these droplets and air flow resistance near walls reduces quickly. With the increase of scrubber diameter, the air flow rate increases and air trends to flow through the areas near walls. Thus, this part of fluid could not contact with droplets adequately and the temperature drop decreases drastically.

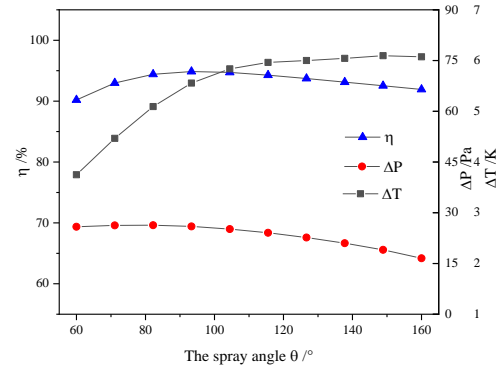


Fig.6 Effects of the spray angle on output parameters

3.5 Interaction effects of input parameters

In order to investigate the influencing degree of different parameters on the performance of scrubber, the local sensitivity analysis is shown in Fig. 7 (where the sprayer height, scrubber diameter and spray angle are 2m, 1m, 100°, respectively).

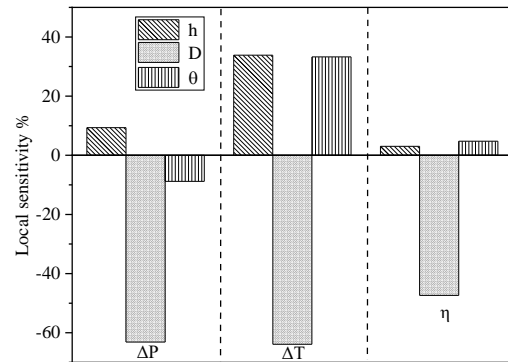


Fig.7 The local sensitivity of design parameters

From the figure, we seem to conclude that the scrubber diameter is the most important parameter for pressure drop, temperature drop and particle removal efficiency. For pressure drop, the local sensitivity of sprayer height and spray angle are +9.33% and -8.81%, which demonstrates that the sprayer height has the greater effects on the pressure drop but the spray angle has negative correlation and sprayer height has positive. For temperature drop, the effects of sprayer height are similar to that of spray angle. For particle removal

efficiency, the spray angle has greater effects than sprayer height.

3.6 Optimization results

In table 2, the comparison between the original design and optimized structures was performed to demonstrate the effectiveness of optimization configuration. Compared with the original design, the particle removal efficiency and temperature drop of optimized structure 2 increase by 3.33% and 15.85%, respectively. Compared with the original design, the particle removal efficiency and temperature drop of optimized structure 3 increase by 4.66% and 17.42%, respectively. The MOGA can trade off multiple objectives and find the optimal points, which can provide some guidance for the optimization of operating conditions.

Table 2 The original design and three optimized structures based on objective functions

items	original design	optimized structure 1	optimized structure 2	optimized structure 3
h/m	2.00	2.00	2.00	3.00
D/m	1.00	0.66	0.66	0.77
$\theta / ^\circ$	100.00	159.88	149.72	105.02
$\eta / \%$	94.84	97.31	98.00	99.26
$\Delta P / \text{Pa}$	25.52	31.65	35.18	41.75
$\Delta T / \text{K}$	5.74	6.66	6.65	6.74

4. CONCLUSIONS

In this study, the Euler-Euler-Lagrange numerical method was developed to predict the performance of wet scrubber. Then the optimization on geometrical parameters of wet scrubber has been performed using genetic aggregation response surfaces and multi-objective genetic algorithms. The conclusions can be summarized as follows:

1. With the increase of sprayer height, the particle removal efficiency pressure drop, and temperature drop rise up. But when the height is larger than 2.5m, the performance of wet scrubber almost stabilizes.
2. When the scrubber diameter increases, the particle removal efficiency pressure drop, and temperature drop reduce rapidly. The scrubber diameter has greatest effects on the performance of wet scrubber.
3. The particle removal efficiency firstly increases and then decreases when the spray angle increases gradually due to the effects of wall film.
4. The comparison between the original design and optimized structures reveals that the particle removal efficiency and temperature drop increase by 4.66% and 17.42%, respectively.

ACKNOWLEDGEMENT

This work is supported by the National Natural Science Foundation of China (No. 51676146).

REFERENCE

- [1] Jinhuang Feng, Huohu Chen, et al. Analysis of dedusting influencing factors and effect of sprayer in desulphurization system. *Environment Engineering* 2010, 28: 70-72.
- [2] Xiaowei Liu, Yishu Xu, et al. Field Measurements on the Emission and Removal of PM_{2.5} from Coal-Fired Power Stations: 1. Case Study for a 1000 MW Ultrasupercritical Utility Boiler. *Eenergy fuels* 2016, 30: 6547-6554.
- [3] B. Raj Mohan, B.C. Meikap. Performance characteristics of the particulates scrubbing in a counter-current spray-column. *Separation and Purification Technology* 2008, 61(1):96-102.
- [4] Qirong Wu, Min Gu, et al. Synergistic removal of dust using the wet flue gas desulfurization systems. *Royal Society Open Science* 2019, 6(7): 181696.
- [5] Danping Pan, Conghui Gu, et al. Investigation on the relationship between slurry drop-let entrainment and fine particle emission in the limestone-gypsum WFGD system. *Energy Sources, Part A: Recovery, Utilization, and Environmental Effects* 2019, 42(14): 1691–1704.
- [6] Samira Lotfi, Weiguo Ma, et al. A wet packed-bed scrubber for removing tar from biomass producer gas. *Fuel Processing Technology* 2019, 193: 197-203.
- [7] Mohammad Javad Jafaria, Amir Hossein Matin, et al. Experimental optimization of a spray tower for ammonia removal. *Atmospheric Pollution Research* 2018, 9: 783-790.
- [8] Zhen Chen, Changfu You, et al. The synergetic particles collection in three different wet flue gas desulfurization towers: A pilot-scale experimental investigation. *Fuel Processing Technology* 2018, 179: 344-350.
- [9] Lung, Cheng. Collection of Airborne Dust by Water Sprays. *Industrial & Engineering Chemistry Process Design & Development* 1973, 12(3): 221-225.
- [10] A. Mohebbi, et al. Simulation of an orifice scrubber performance based on Eulerian/Lagrangian method. *Journal of Hazardous Materials* 2003, 100: 13-25.
- [11] Ali Majid, Yan Changqi, et al. CFD simulation of dust particle removal efficiency of a venturi scrubber in CFX. *Nuclear Engineering and Design* 2013, 256: 169-173.
- [12] K.S. Lim, S.H. Lee, H.S. Park. Prediction for particle removal efficiency of a reverse jet scrubber. *Journal of Aerosol Science* 2006, 37(12): 1826-1839.